Surface Potential, Field-Effect Mobility, and Surface Conductivity of ZnO Crystals

H. J. KRUSEMEYER
Bell Telephone Laboratories, Murray Hill, New Jersey
(Received December 4, 1958)

Measurements of surface properties of ZnO crystals were made at 300°K, both in dry O_2 and in high vacuum. The dark conductivity was changed by illumination with ultraviolet. Surface potentials of crystals with diameters down to 0.002 cm were measured by the Kelvin method with a sensitivity of 0.002 v. Comparison of the measured and calculated dependence of dark conductivity on dark surface potential showed that the latter could be changed from about 0.1 v below to 0.5 v above the neutral point. Application of a transverse electric field produces a fast change in conductivity in less than 50 μsec and a slow change in which part of the fast change decays with a time constant ranging from minutes to hours depending on ambient and surface potential. The field effect mobility increases with increasing surface potential from a value which is sometimes smaller than one to a plateau value between 70 and 145 cm^2v^{-1} sec^{-1} and decreases again for the largest value of surface potential. Evidence is given that the low mobility values are caused by surface states. Combined measurements of surface potential, field-effect mobility, and surface conductivity together with quantum efficiency measurements of the surface conductivity by Collins and Thomas yield the quantum efficiency of the hole-trapping process at the surface which is approximately 1 for a neutral surface. A quantitative treatment of the hole-trapping process is in good agreement with the experimental results and shows that the bulk diffusion length for holes is >1000 A and that the ratio of hole surface trapping velocity and diffusion constant equals 1.7×10^5 cm^{-1}.

INTRODUCTION

IT has been shown by Mollwo and co-workers[1] and Miller and co-workers[2] that the dark conductivity of ZnO is increased after illumination with ultraviolet (uv). The increase decays slowly in the dark with a rate depending on the partial pressure of the surrounding gases. The holes created by the uv are assumed to diffuse to the surface where they can be trapped. These authors assumed the traps to consist of adsorbed oxygen ions which thus are neutralized causing an increased density of conduction electrons in the space charge layer. As the change in dark conductivity of single crystals is too large to be explained by photo-desorption of oxygen from a surface which is neutral without adsorbed oxygen ions, Heiland[3] has suggested that the clean surface is positively charged either because of surface states or a higher density of donors in the skin than in the bulk of the crystal. Another mechanism which allows the surface to become positive after exposure to uv is that the holes are trapped by surface oxygen lattice ions as well as adsorbed oxygen ions as has been mentioned by Heiland[3] and discussed in more detail by Collins and Thomas.[4,5] Mollwo[1] has reported a second process attributed to changes in the bulk whereby the conductivity changes much faster after a change in light intensity. As this effect was at least negligibly small in our experiments, we shall use henceforth "conductivity" instead of "dark conductivity." The results to be presented here[6] show that the surface potential can be changed over a large range, which includes the neutral point, by illumination with uv and this we have used as a means for studying the dependence of surface conductivity and field effect mobility on surface potential. This dependence was the same in oxygen and in vacuum whether the crystal is illuminated or not. In turn some of these results give additional information about the hole trapping process at the surface.

EXPERIMENTAL ARRANGEMENT

The needle-shaped hexagonal ZnO crystals (wurtzite structure) were grown by Thomas according to the Scharowsky[7] method and kindly made available to us. Figure 1 shows such a crystal of a few mils diameter mounted in the coaxial holes filled with Ga, in the end of two Pt rods *b*. The Kelvin method was used for measuring changes in the surface potential of the crystal. The $\frac{1}{8}$-in. long reed *d* consisted alternatively of 0.025 cm Pt+10% Rh and 0.005 cm W wire which was spotwelded to a lever which in turn was attached to a spring *f*. The spring is excited by an electromagnet mounted outside the vacuum system, which causes the reed wire to pass back and forth in a plane parallel to the crystal and at a distance of about 0.002 cm from it. The crystal could be illuminated from the side of the reed with virtually parallel light during the intervals that the reed was not passing between light source and crystal. Consequently, the surface of the reed facing the crystal is not directly exposed to uv and thus the potential of this reed surface is not changed by illuminating the crystal. This way the uncertainty about the stability of the reed surface potential which exists when a change in ambient is used to change the crystal surface potential, is avoided. The change in the dc potential between reed and crystal required to keep the ac potential zero is the quantity actually measured. As the mounting rods holding the crystal had a tendency to vibrate with very small amplitude because of the re-

[1] E. Mollwo, *Proceedings of the Conference on Photoconductivity*, Atlantic City, November 4–6, 1954, edited by R. G. Breckenridge *et al.* (John Wiley & Sons, Inc., New York, 1956), p. 509.
[2] P. H. Miller, *Proceedings of the Conference on Photoconductivity*, Atlantic City, November 4–6, 1954, edited by R. G. Breckenridge *et al.* (John Wiley & Sons, Inc., New York, 1956), p. 287.
[3] G. Heiland, Z. Physik **142**, 415 (1955).
[4] R. J. Collins and D. G. Thomas, Bull. Am. Phys. Soc. Ser. II, **2**, 27 (1957).
[5] R. J. Collins and D. G. Thomas, Phys. Rev. **112**, 388 (1958).
[6] H. J. Krusemeyer, Bull. Am. Phys. Soc. Ser. II, **3**, 218 (1958).
[7] E. Scharowsky, Z. Physik **135**, 318 (1953).

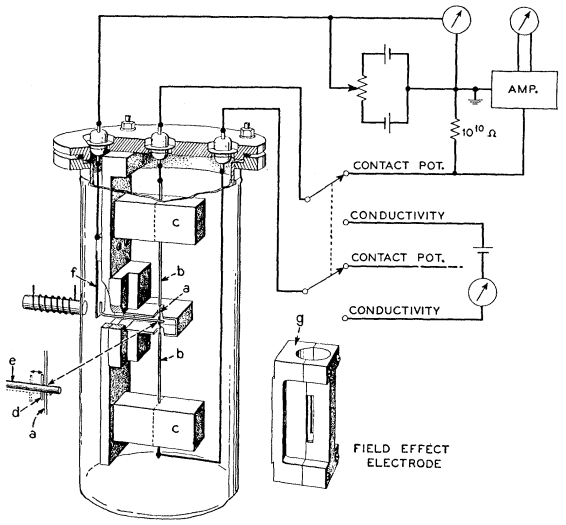

FIG. 1. Apparatus for measuring conductivity, surface potential, and field effect mobility. (a) crystal, (b) support wires, (c) ceramic blocks, (d) reed, (e) lever, (f) leaf spring, (g) field effect electrode.

action forces of the vibrating parts on the apparatus and as the input impedance of the tuned ac amplifier used had to be high (10^{10} ohms), the electrostatic charges located on the inside of the glass tubing of the vacuum system and on the insulators holding the mounting rods introduced a relatively large error signal. This was eliminated by covering these parts with platinum foil, not shown in Fig. 1, except for a small opening passing the light. A criterion for proper operation of the apparatus is that the results are independent of the amplitude of the vibrating reed. For a 1-mil diameter crystal a change of 2 mv in surface potential could be detected.

To measure the field-effect mobility, the reed and associated shielding were removed and the metal cylinder g with 1 cm inside diameter and consisting of two parts, was placed around the crystal without disturbing its contacts. Two slots in the cylinder wall 0.25 cm wide were provided for illuminating the crystal from opposite sides. Because of the small diameter of the crystals, no dielectric was required between crystal and field effect electrode. For a crystal with a diameter as large as 10^{-2} cm, a field-effect voltage of 1000 volts gives a field at the crystal surface equal to that caused by 10^{-4} monolayer of charge. That the transverse electric field at the edges of the crystal is higher than in the middle of a face does not introduce any errors provided the transverse field is in the range where field effect mobility does not depend on the magnitude of the transverse field. As the crystals were not long enough to accommodate four probes for measuring conductivity during contact potential measurements, the current contacts and homogeneity of the crystal were first checked for different values of the conductivity with the four probe technique. During the actual measurements, the conductivity was obtained by measuring the voltage across the whole crystal and the current through it. Only crystals which were homogeneous over the entire range of conductivity and which did not show a voltage drop across the current contacts were used.

RESULTS

A constant transverse electric field of either polarity could be applied or removed between the field cylinder g and the crystal within a few microseconds but the resulting change in the conductivity of the crystal could be measured only 50 μsec after that. Within this time the maximum change in conductivity took place. Part of this change decays again with a time constant ranging from minutes to hours depending, as the magnitude of the decay did, on the surface potential of the crystal and the pressure of the surrounding gas. We shall discuss this in more detail in the last section.

In Fig. 2 is shown the field-effect mobility as a function of the conductivity σ of a crystal obtained by illumination with different quantities of uv. The field-effect mobility μ_f, as has generally been accepted, is the average mobility of the charges on the crystal surface and in the space-charge layer which screen the applied transverse electric field from the interior of the crystal. It refers below always to the initial change in conductivity which persists for at least seconds after a change in transverse field.

To obtain the point with the lowest mobility in Fig. 2, the crystal was first exposed to dry oxygen in the dark until a steady state was reached. Subsequently it was kept in a vacuum of 10^{-6} mm Hg until a new steady state was reached which for the conductivity happened to be close to the one in dry oxygen. For successive points, the field-effect mobility and conductivity were measured after exposing the crystal to increasing quan-

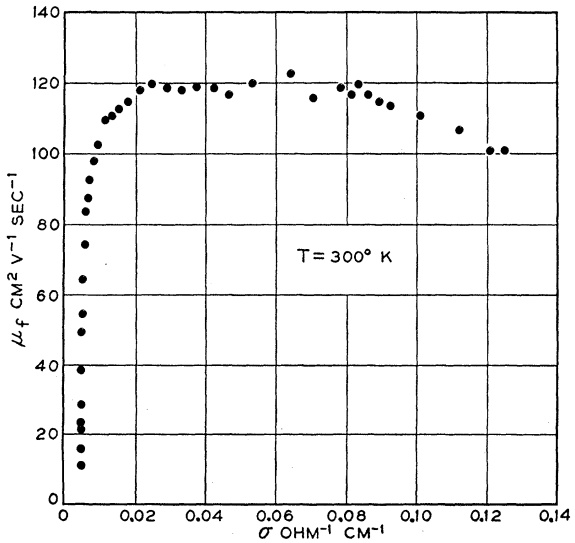

FIG. 2. Field effect mobility as a function of conductivity.

tities of uv in a vacuum of 10^{-6} mm Hg. For the same value of conductivity μ_f was the same, whether the crystal was still exposed to uv or not. The results were not changed either by measuring the point with the highest conductivity first and successive points while the conductivity was slowly decaying. In one atmosphere of oxygen the maximum obtainable value for the conductivity is appreciably lower than in vacuum, the minimum value only slightly lower. In the overlapping conductivity range the mobility results are identical. The smallest mobility value in oxygen is about 25% lower than the smallest value in vacuum which occurs for a slightly higher conductivity. In order to see if the mobility would increase again for larger negative surface potentials, it has been attempted to increase the range of the data using large negative field-effect voltages while the crystal had its lowest conductivity. The results were, however, irreproducible as the large voltages seemed to change the crystal surface, possibly by ion bombardment. The main features of the curve in Fig. 2 are an initial rapid rise in mobility until a plateau is reached and a much slower drop for the largest values of the conductivity. Very recently Heiland[8] published field-effect data on ZnO crystals taken at 90°K which showed only the rapid increase without the plateau and slow drop following it. The highest field-effect mobility value obtained by Heiland was 30 $cm^2v^{-1}sec^{-1}$.

For different crystals we found the shape of the curves to be very similar though the plateau value of the mobility ranged from 75 to 145 $cm^2v^{-1}sec^{-1}$. The mobilities for the lowest value of the conductivity ranged from about 0.1 to 50 $cm^2v^{-1}sec^{-1}$ with in general the lower mobility for crystals with the lower bulk conductivity. Values below 5 were only found for crystals for which the bulk conductivity was decreased by doping[5] with lithium. Some evidence will be presented in a later section that the main cause for the low mobility values for small values of the conductivity are surface rather than bulk levels. The surface potential in the plateau region changes over many kT/e as will be shown later. Because of this it will be assumed from here on that no screening of the transverse field by surface states takes place in the plateau region and that the micromobility of the electrons equals the plateau value of the field-effect mobility. This is 120 $cm^2v^{-1}sec^{-1}$ for the crystal of Fig. 2 and is rather close to the value of 150 $cm^2v^{-1}sec^{-1}$ obtained from Hutson's[9] Hall data using the factor $\frac{3}{8}\pi$. It may be pointed out that surface roughness on a scale larger than the thickness of the space charge layer and in the path of the electrons moving in the direction of the c axis would give a lower value for the field-effect mobility without changing the shape of the curve. If this is what takes place it is for what follows as well to equate the plateau value of the field-effect mobility

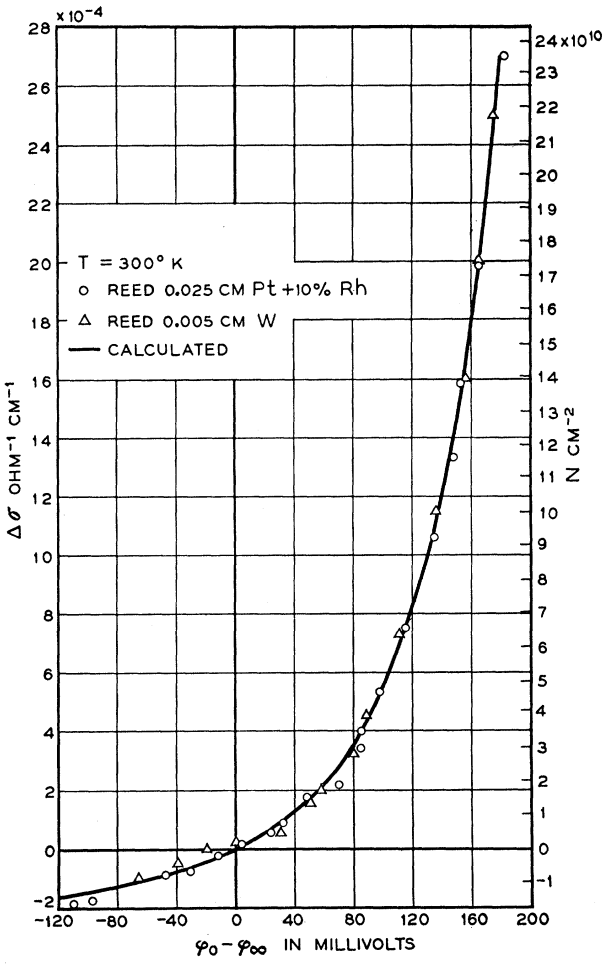

FIG. 3. The dependence of surface charge density on surface potential.

to the micromobility as to correct the length of the crystal. It was noted that the plateau value of the mobility could be changed by etching the crystal.

The points in Fig. 3 give the measured dependence between the change in conductivity and surface potential for the non-Li doped crystal of Fig. 2. The circles were obtained using the 0.025-cm diameter Pt+10% Rh reed and the triangles using the 0.005 cm W reed, both after correction for nonuniform illumination of the crystal as discussed in Appendix I. The correction was the same for both reeds.

The solid curve in Fig. 3 represents the calculated relation[10]

$$N=\pm\left[\frac{kT\epsilon n_\infty^-}{2\pi e^2}\right]^{\frac{1}{2}}\{-1-e(\varphi_0-\varphi_\infty)/kT+\exp[e(\varphi_0-\varphi_\infty)/kT]\}^{\frac{1}{2}}, \quad (1)$$

in cgs units, between the density of surface charges N

[8] G. Heiland, J. Phys. Chem. Solids **6**, 155 (1958).
[9] A. R. Hutson, Phys. Rev. **108**, 222 (1957).
[10] H. J. Krusemeyer and D. G. Thomas, J. Phys. Chem. Solids **4**, 78 (1958).

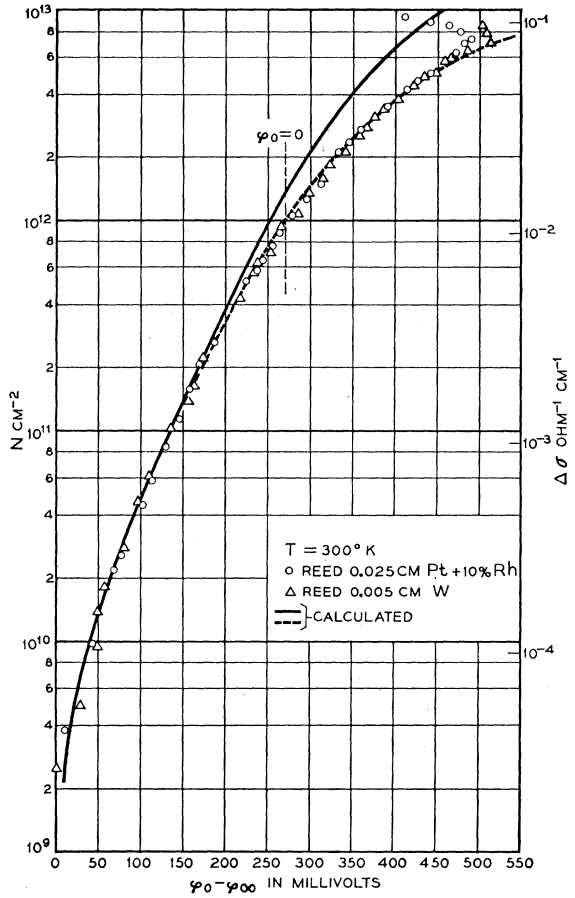

FIG. 4. The dependence of surface charge density on surface potential.

and the barrier height $\varphi_0-\varphi_\infty$ of the space charge layer assuming that all the donors are ionized in the field-free interior and that a negligible density of acceptors exists in the bulk. n_∞^- is the density of conduction electrons in the field free interior of the crystal. The dielectric constant $\epsilon=8.5$ as was found by Hutson[9] using single crystals. The density of surface charges in Fig. 3 is related to the change in the conductivity of the crystal by the assumed micromobility of 120 $cm^2v^{-1}sec^{-1}$ for electrons. The measured points were made to fall on the calculated curve by translation only and in this way the neutral point of the crystal surface was determined both for surface potential and surface charge density. As (1) is dependent on n_∞^-, which in turn can only be determined when the neutral point is known, one may proceed as follows. As a first approximation n_∞^- is derived from the conductivity of the crystal after it has been in the dark and in oxygen for a long time, assuming a homogeneous density of carriers right up to the surface. The error is small as the surface is now negative without an inversion layer (3.2-ev band gap[11]). For this value of n_∞^- the dependence between N and $\varphi_0-\varphi_\infty$ using (1) is compared with the data and the neutral point obtained. The conductivity of the crystal at this point yields a new value for n_∞^- for which (1) is replotted, etc. The second value of n_∞^- is in most cases already accurate enough as a change of n_∞^- in (1) by a factor of two changes by less than 2% the value of n_∞^- obtained by fitting the experimental data to the calculated curve. The corresponding shift in neutral point is about kT/e volt. This makes the evaluation of the neutral point rather accurate and only slightly dependent on the assumed micromobility of 120 cm^2v^{-1} sec^{-1}. For the crystal of Fig. 3 $n_\infty^-=2.27\times10^{14}$ cm^{-3}.

We notice in Fig. 3 that the surface does not become more than about 120 mv negative and carries less than 10^{-4} monolayer of negative charge including that in surface states. Figure 4 gives a continuation of these results for higher densities of positive surface charge. The solid curve gives again the calculated dependence between density of surface charge and barrier height of the space charge layer which below $\varphi_0=0$ is given by (1). For $\varphi_0=0$ the Fermi level crosses the conduction band edge at the surface and part of the electron gas in the space-charge layer becomes degenerate giving rise to the curvature on the top of the graph. In this region the following relations instead of (1) give the dependence of the density of surface charge on barrier height.[10] For $e\varphi_0\leq 0$,

$$N=K^{\frac{1}{2}}\left[-\frac{\pi^{\frac{1}{2}}n_\infty^-}{2N_c}-\frac{\pi^{\frac{1}{2}}}{2}\sum_{n=1}^{\infty}(-1)^n n^{-\frac{5}{2}}\exp n\beta_0\right]^{\frac{1}{2}};$$

for $e\varphi_0>0$,

$$N=K^{\frac{1}{2}}\left[-\frac{\pi^{\frac{1}{2}}}{2}\left(\frac{n_\infty^-}{N_c}\right)+\frac{\pi^2}{6}\beta_0^{\frac{1}{2}}+\frac{4}{15}\beta_0^{\frac{5}{2}}+\sum_{n=1}^{\infty}(-1)^n n^{-\frac{5}{2}}\times\left\{\exp(-n\beta_0)\int_0^{\sqrt{(n\beta_0)}}\exp y^2 dy-\exp(n\beta_0)\int_{\sqrt{(n\beta_0)}}^{\infty}\exp(-y^2)dy\right\}\right]^{\frac{1}{2}},$$

where $\beta_0=e\varphi_0/kT$. φ_0 is the electrostatic potential at the surface if the Fermi level has zero potential. N_c is the effective density of states in the conduction band. $K=(2\epsilon/e^2h^3)(2m^*)^{\frac{3}{2}}(kT)^{\frac{5}{2}}$. Hutson's[9] value of $\frac{1}{2}$ for the ratio of the effective to the free electron mass m^*/m has been used. These expressions have been derived assuming spherical energy surfaces at the bottom of the conduction band and using Fermi statistics.

The circles in Fig. 4 were obtained using the 0.025 cm diameter Pt+10% Rh reed and the triangles using the 0.005 cm W reed. For large surface charge density, the barrier height seems to decrease again. This is caused by a change in the surface potential of the reed because of scattered light. Thus, when a reflecting surface was placed behind the crystal, causing a much

[11] E. Mollwo, Z. angew. Phys. 6, 257 (1954).

larger fraction of the uv to fall on the surface of the vibrating reed facing the crystal, the rather sharp kink was replaced by a much more gradual bend which sets in at about a 200 mv lower value for $\varphi_0-\varphi_\infty$, as is expected from the following argument. To raise the value of N from 6×10^{12} cm^{-2} to 8×10^{12} cm^{-2} requires about a ten times longer exposure to uv than to change N from 0 to 6×10^{12} cm^{-2}, as at a coverage of about 10^{13} the trapped hole production rate at the surface by the uv equals the loss rate. Thus, if the amount of scattered light is large as with the mirror, a detectable error in contact potential starts at a lower crystal surface potential, and increases much more slowly with increasing surface potential than when the amount of scattered light is small, the case shown in Fig. 4. It will be noted in Fig. 4 that, to change their surface potential, more light is required for the tungsten than for the platinum reed.

In deriving the dependence between N and $\varphi_0-\varphi_\infty$, the surface charges were assumed to be located exactly at the vacuum crystal interface. If the positive charge consists however of adsorbed ions, their average distance from the surface will have a finite value and will give rise to an increased barrier height. These adions may be the zinc ions discussed by Collins and Thomas,[5] which are left behind when oxygen lattice ions trapping a hole are desorbed. If the positive surface charge is located at an average distance of 0.94 A from the surface, which corresponds with a dipole moment of 1.5×10^{-27} coulomb cm per adion, the broken line in Fig. 4 is obtained which fits the data surprisingly well considering the many complications to be expected for very large densities of surface charge.

The measured dependence between the field effect mobility and conductivity as shown in Fig. 2 and the dependence between surface potential and conductivity as shown in Figs. 3 and 4 can be combined to give the mobility as a function of surface potential as shown by the dots in Fig. 5. This is easily done as the electrical contacts on the crystal are not disturbed when the apparatus is modified between surface potential and field effect measurements. One notices that the largest value for the mobility is obtained for $\varphi_0>0$. This is when the electron gas near the surface has already become degenerate. There is no appreciable reduction in the mobility caused by increased scattering when the conduction electrons become confined to a narrow channel,[12] though the slight decrease in mobility shown in Fig. 2 for larger values of conductivity may possibly be attributed to this. This region of decreasing mobility is not shown in Fig. 5 as, because of reed surface potential changes by the light, no reliable contact potential data are available in this range.

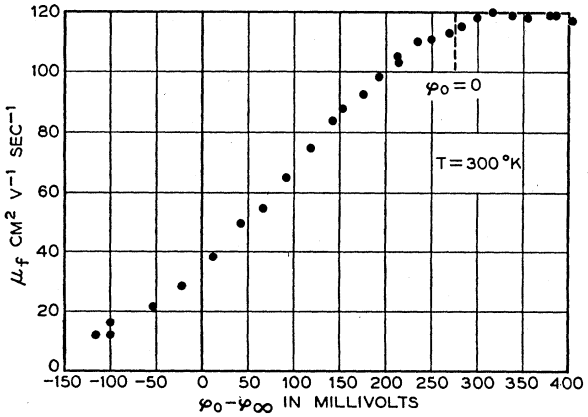

FIG. 5. Field-effect mobility *versus* surface potential.

DISCUSSION OF RESULTS

The field-effect mobility is given by

$$\mu_f=\mu_m\left\{d\int_0^\infty n_\infty^-\left[\exp\left(\frac{e(\varphi-\varphi_\infty)}{kT}\right)-1\right]dx\right\}\Big/ \times d(\sum N_1+\sum N_2+F), \quad (2)$$

where μ_m is the micromobility of the electrons, and φ is the electrostatic potential at a distance x from the surface

$$N_1=\frac{N_{10}}{1+\exp[-e(\psi^+ +\varphi_0-\varphi_\infty)/kT]}, \quad (3)$$

is the density of electrons in donor-type surface states with a density N_{10} and an electron energy $-e\psi^+$ above the Fermi level when the surface is neutral.

$$N_2=\frac{N_{20}}{1+\exp[-e(\psi^- +\varphi_0-\varphi_\infty)/kT]} \quad (4)$$

is the density of electrons in acceptor surface states with a density N_{20} and an energy $-e\psi^-$ above the Fermi level when the surface is neutral. $\sum N_1$ and $\sum N_2$ represents the total contribution of different levels. The total space charge per cm^2 of surface area expressed in units of the electronic charge[10] is given by

$$F=\pm[kT\epsilon/2\pi e^2]^{\frac{1}{2}} \times[n_\infty^-(-1+\lambda)+\textstyle\sum_i N_{di}[\ln(\alpha_i-1+\lambda^{-1})-\ln\alpha_i] +\sum_i N_{ai}[\ln(\beta_i-1+\lambda)-\ln\beta_i]]^{\frac{1}{2}}. \quad (5)$$

The plus sign is used for positive surface potentials only. $\lambda=\exp[e(\varphi_0-\varphi_\infty)/kT]$, N_{di} is the bulk donor density of which a fraction $1/\alpha_i$ is ionized in the field-free interior, and N_{ai} and $1/\beta_i$ are these quantities for acceptors. Neutrality in the field-free interior requires, of course, that $n_\infty^-+\sum(N_{ai}/\beta_i)=\sum(N_{di}/\alpha_i)$. If we choose φ rather than x as the variable in the integral of (2), this expression can be simplified to

$$\mu_f=\frac{\mu_m\epsilon n_\infty^-\{\exp[e(\varphi_0-\varphi_\infty)/kT]-1\}}{4\pi e(d/d\varphi_0)(\sum N_1+\sum N_2+F)}. \quad (6)$$

[12] J. R. Schrieffer, Phys. Rev. **97**, 641 (1955).

It is an easy matter to combine (6) with (3), (4), and (5) to obtain μ_f as a function of barrier height $\varphi_0-\varphi_\infty$. Using this expression it can be shown that the mobility in Fig. 5 does not change rapidly enough with barrier height to be explained by just one or two surface levels while neglecting immobile screening charge in the space-charge layer. The use of (6) requires that the total density of filled and empty surface states with a particular energy be independent of the illumination. It is, however, quite possible that this density is changed by irradiation with uv.

The evaluation of the neutral point in Fig. 3 and therefore the zero of the potential in Fig. 5 (however not the shape of the curve) were based on the assumption that all the donors were ionized in the field free interior and that acceptors could be neglected. It can be asked if the low mobility for small values of the conductivity in Fig. 2 is not caused partly or wholly by screening of the transverse field by immobile charges in the space charge layer rather than by surface states. For this reason, a set of bulk levels was constructed with the help of (5) and (6) which gave roughly the mobility dependence of Fig. 5. For these bulk properties, the density of surface charges as a function of barrier height was calculated using (5), and from this the dependence of the change in conductivity $\Delta\sigma$ in Fig. 3 on barrier height. In this last step, the calculated dependence of field-effect mobility on barrier height for the assumed bulk properties was used rather than the experimental results of Fig. 5. The same calculations were done for another non-Li doped crystal. The results of both coincide for higher values of surface potential (field-effect mobility$\approx$micromobility) with the solid line in Fig. 4, as in this region the immobile charge in the space-charge layer does not contribute significantly to the space charge. For lower surface potentials, particularly when there is a depletion layer, the new dependence stayed well above the solid line in Fig. 3 as is easily visualized. If the immobile screening charges are right at the surface the electric field terminating on them and originating from charge put on the surface does not contribute to the barrier height of the space-charge layer. If, however, these charges are in the space-charge layer the opposite is true. It was not possible to match the surface potential data to the new dependence even by translation. Thus, it appears that at least the major cause for the low field-effect mobilities for the non-Li doped crystals are surface states.

SURFACE TRAPPING OF HOLES

In this section the quantum efficiency will be calculated of the hole-trapping process for a positively charged or neutral surface, without assuming that the bulk diffusion length for holes is large with respect to the thickness of the space charge layer. The results will be compared with experiment by combining the quantum efficiency data of Collins and Thomas[5] with the field-effect mobility and surface potential measurements described here. Collins and Thomas measured the number of incident photons per cm^2 of surface area, required to increase the lowest value of conductivity to a specific value. Assuming a micromobility value of 100 cm^{2}v^{-1}sec^{-1}, they presented the results as the increase of the number of conduction electrons in the space charge layer per unit of surface area as a function of the required number of photons. In Fig. 6, p^+ is the increase in the density of holes trapped at the surface over the density already present when the surface was neutral and q is the total number of photons per cm^2 required to give rise to p^+. The points in this figure were obtained from the data in Fig. 6 of the paper by Collins and Thomas, by multiplying their number of electrons in the space charge layer with $\mu_f/100$ and correcting for the neutral point which we obtained on the same crystal. The Collins and Thomas experiment was done for three different light intensities. Different points for the same intensity were obtained by varying the exposure time. In order to calculate p^+ as a function of q, we will imagine that the illumination of the crystal takes place by exposing it successively to short flashes of light. The intensity of a flash is so small that the resulting concentration of holes outside surface traps does not influence significantly the potential distribution in the space charge layer which is thus only determined by the bulk properties of the crystal and the charge density at the very surface. The flashes are short enough for the trapped holes produced at the surface by one flash not to change the surface charge significantly. Thus it is only necessary to describe the transport of holes during and after one flash while the density of surface charge is constant, but as a function of this density. In each point of the crystal the electrons in the conduction band are assumed to be in thermal equilibrium among themselves and so are the electrons in the valence band. There is, however, not necessarily equilibrium between these two groups of electrons and the electrons in the trap and recombination levels. The following assumptions will be made about the bulk recombination centers. The density has to be large enough and the lifetime of a captured hole

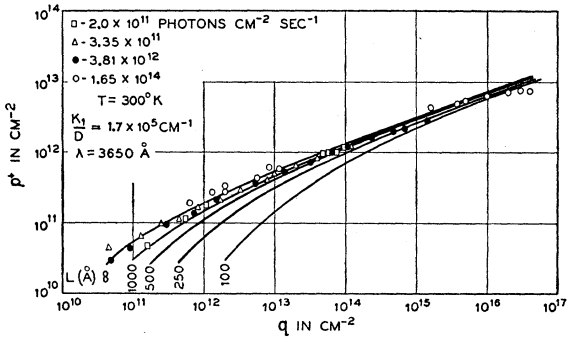

FIG. 6. Relation between total number of incident photons and increase in the density of trapped holes.

small enough to allow the density of centers without a hole to be constant throughout the crystal independent of the local electrostatic potential and for all time. We will assume too a large enough energy difference between the recombination centers and the top of the valence band and intense enough flashes of uv for the Fermi energy of the recombination centers to be at least a few kT above the Fermi energy for the valence band as long as the density of free holes cannot be neglected. These assumptions will make, according to the Shockley-Reed model,[13] the hole lifetime τ because of bulk recombination, constant in space and time. The continuity equation at a distance x from the surface may be written as

$$\frac{\partial p}{\partial t}=D\frac{\partial^2 p}{\partial x^2}+\mu\frac{\partial[p\partial\varphi/\partial x]}{\partial x}-\frac{p}{\tau}, \tag{7}$$

where p, D, and μ are respectively the concentration, diffusion constant, and mobility of holes. φ is the electrostatic potential. As the trapped holes at the surface decay very slowly in a vacuum or even in one atmosphere of dry oxygen one may conclude that the transfer of holes from surface traps to the valence band can be neglected during a flash. Thus the boundary condition for the solutions of (7) can be written as

$$I_0=-D\left(\frac{\partial p}{\partial x}\right)_0-\mu p_0\left(\frac{\partial\varphi}{\partial x}\right)_0=-K_1 p_0, \tag{8}$$

where I is the hole flux. The subscript zero indicates $x=0$ and K_1 is the surface trapping velocity. K_1 is proportional to the density of empty surface traps and thus depends on the surface charge density. However K_1 may be regarded as constant for one flash if its duration is short enough. For the boundary condition at a large distance x_1 from the surface will be taken

$$p_{x_1}=0. \tag{9}$$

As (7), (8), and (9) are linear in the hole density p, we may assume that the holes of one flash are produced instantaneously, which gives for the free hole density at $t=0$

$$p(0)=p_0(0)\exp(-\alpha x), \tag{10}$$

α is the absorption constant of the uv.

By solving Poisson's equation under the assumption that the space-charge density equals the density of conduction electrons, and by expressing the surface field in the surface charge density, one finds for the dependence of $\partial\varphi/\partial x$ on x and the density of surface charges N

$$-\frac{\partial\varphi}{\partial x}=\frac{2kT/e}{k_1/N+x}, \tag{11}$$

with $k_1=kT\epsilon/2\pi e^2$ and in cgs units. Equation (11) holds provided that $e(\varphi-\varphi_\infty)/kT\geq 2$ and that the crystals are not highly compensated. That the last point applies to the crystals used in this study was shown in the previous section. To simplify the calculation it is assumed that (11) is a good approximation for the electric field throughout the crystal. However, it is only important that it holds in a region from which holes can reach the surface as we are only interested in the hole concentration at the surface. From the solution of (7), (8), (9), (10), and (11) p_0 is found in Appendix II as a function of t, $p_0(0)$ and α. From this the quantum efficiency is derived for the surface charge-producing process as a function of barrier height, and finally the following relation between p^+ and q of Fig. 6 is obtained:

$$q=\int_0^{p+}\frac{D(\alpha+L^{-1})[(K_1/D)+L^{-1}+\gamma^{-1}(\alpha+L^{-1})]}{K_1\alpha\gamma\exp(\gamma)\int_\gamma^\infty\exp(-z)dz/z}d\zeta, \tag{16}$$

with

$$\gamma=(\alpha+L^{-1})k_1\Big/\int_0^\zeta\frac{\mu_f}{\mu_m}dp^+,$$

μ_m is the electron micromobility and L is the hole bulk diffusion length. K_1 is not constant if the number of available trapping sites is decreasing materially with increasing values of p^+. According to measurements done by Mollwo[1] on films of ZnO, the absorption constant $\alpha=2.5\times10^5$ cm^{-1} for $\lambda=3650$ A, the wavelength used by Collins and Thomas. Consequently this value has been used for plotting the solid lines in Fig. 6 which represent (16) for different values of the diffusion length and a constant value of K_1. One notices especially for the smaller diffusion length that p^+/q is constant for small values of p^+. In this region of low barrier height of the space-charge layer, the quantum efficiency is determined by the diffusion length rather than by the barrier height. The smaller L is, the larger is the barrier height for which this behavior persists. For large barrier height the quantum efficiency becomes practically independent of diffusion length as indicated by the converging of the curves. Comparison with the experimental points indicates that the bulk diffusion length of holes for this crystal is not smaller than 10^{-5} cm and that $K_1/D=1.7\times10^5$ cm^{-1}. As the diffusion constant for holes is not likely to be larger than for conduction electrons, $K_1\leq5\times10^5$ cm sec^{-1}. One notices that for higher values of p^+ the experimental points seem to level off more than the calculated curves. This is expected to happen for the following reasons. It was assumed in integrating (16) that the concentration of trapped holes at the surface does not decay during the experiment. However, in order to obtain the largest p^+ values, the exposure time in the Collins-Thomas experiment became long enough for some decay to take place.

SLOW FIELD EFFECT

As the time constant of the decay of the change in conductivity caused by a transverse electric field is

[13] W. Shockley and W. T. Reed, Phys. Rev. 87, 835 (1952).

rather long and the amplitude rather small, the effect can only be observed when the crystal is either in the steady state in the dark or in the steady state during constant illumination. In the second case, the rate of arrival of holes which are trapped at the surface equals the loss rate of holes already trapped. If a transverse field is now applied, the sign of the change in the rate of arrival of holes is always opposite to the change in the number of electrons in the space-charge layer. Consequently, the density of trapped holes will try to maintain the surface potential which was present before the field was applied. This explanation can, however, not be advanced when the crystal is in the steady state in the dark. In this case the total density of adsorbed oxygen ions and atoms is possibly a function of surface potential,[10,14] with the adsorption or desorption process being responsible for the long time constant.

CONCLUSIONS

Illumination of a ZnO crystal with uv results in an increased surface potential as well as in increased conductivity. The dependence between surface potential and conductivity is as expected for a surface space-charge layer. Small field-effect mobilities for negative and small positive surface potentials are caused by a distribution of surface states rather than by levels in the space charge layer. Quantitative agreement exists between the quantum efficiency measurements of Collins and Thomas and the model that some of the holes produced by the uv are able to reach the surface where they have a chance of being trapped.

ACKNOWLEDGMENTS

The author is much indebted to M. V. Pursley for selecting the rare crystals which made the experiment possible and for his very competent asistance with the measurements, and to Mrs. E. Ancmon for the numerical computations. Many helpful discussions were had with R. J. Collins and D. G. Thomas.

APPENDIX I

The hexagonal crystal was mounted with one of its faces parallel to the plane of vibration of the reed and perpendicular to the beam of uv. The two faces bordering on and making 60° angles with this face absorb during illumination less than half the amount of light per unit surface area which results in a different surface potential and surface conductivity. The other faces of the crystal receive only scattered light. We shall assume that the reed measures the average of the surface potential of the front face and the potential of the two bordering faces. One can easily convince oneself, with the aid of Fig. 3, that this average potential is approximately equal to the surface potential corresponding with the average of the surface conductivity of these three faces. This seems to be supported too, by the fact that the experimental results were the same using a 0.025-cm and a 0.005-cm reed. Thus if there were no scattered uv falling on the three back faces of the crystal, one could just correct by multiplying the measured change in conductivity by a factor of two. As, however, the quantum efficiency of the hole-trapping process at the surface goes down rapidly with increasing surface charge,[5] the scattered light on the back faces can have a negligible influence on conductivity for low values of the crystal conductivity but may contribute nearly as much as the direct light for large values of conductivity. In order to determine the contribution of the back faces to a conductivity change, the reed in Fig. 1 was replaced by a much longer wire which at rest cut out all but the scattered light falling on the crystal. For each of different amounts of light, the crystal was illuminated both with and without the shadow wire vibrating and the resulting change in conductivity was measured. Before each illumination the conductivity was allowed to decay to its lowest value. We shall assume that the same amount of scattered light is absorbed at every point of the crystal surface, thereby giving rise to a total conductivity change $\delta\sigma$ when the shadow wire is at rest. The conductivity change with the wire vibrating is $\Delta\sigma_1$ and the contribution of the three front surfaces to it $\Delta\sigma_2$. Thus, $\Delta\sigma_1=\Delta\sigma_2+\frac{1}{2}\delta\sigma$ and $\alpha=2-\delta\sigma/\Delta\sigma_1$ where α is a correction factor with which $\Delta\sigma_1$ has to be multiplied to obtain the change in conductivity for a crystal illuminated both from the front and the back and corresponding with the measured change in contact potential. In Fig. 7 results are plotted for the crystal of Figs. 3 and 4. The zero of the ordinate $\Delta\sigma_1=0$ corresponds with the

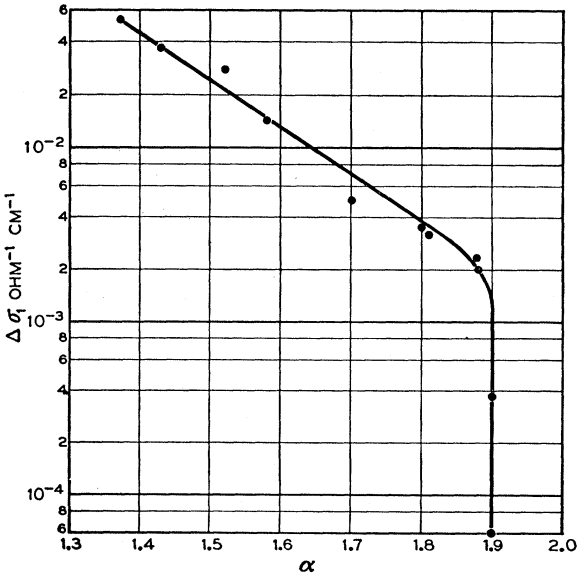

FIG. 7. The correction factor α for inhomogeneous illumination of the crystal *versus* the measured change in conductivity.

[14] P. Aigrin and C. Dugas, Z. Elektrochem. **56**, 363 (1952); K. Hauffe and H. J. Engell, Z. Elektrochem. **56**, 366 (1952); H. J. Engell and K. Hauffe, Z. Elektrochem. **57**, 762 (1953); K. Hauffe, Angew. Chem. **67**, 189 (1955).

steady state of the crystal in the dark. We notice that the correction factor is constant for the whole range of Fig. 3.

It was assumed in the preceding that holes produced on one side of the crystal would not diffuse across or along the surface to the other side. This was confirmed in the following way. Directly after the crystal was strongly illuminated from one side only, it was exposed to the same amount of light which in one experiment came from the same, in a second experiment from the opposite direction.

In the first case the increase in conductivity because of the second illumination was much smaller than in the second case. This is in conformity with the fact that the quantum efficiency of the surface trapping process decreases rapidly with increasing surface charge density.

APPENDIX II

The solution of (7), (8), (9), (10), and (11) is obtained by using the transform $p=v(x+k_1/N)$, where v is a new variable in x and t, and subsequent separation of variables. The solution can be written as

$$p=2(k_1/N+x)\sum_{i=1}^{\infty}\left\{\left[\frac{p_i\xi}{x_1}\cos\frac{p_ix}{x_1}+\sin\frac{p_ix}{x_1}\right]\Big/\left[x_1+2\xi+\frac{p_i^2\xi^2}{x_1}-\left(\frac{p_i^2\xi^3}{x_1^2}+\xi\right)\cos^2p_i\right]\right\}\times B\exp\left\{-\left[\frac{p_i^2}{x_1^2}+L^{-2}\right]Dt\right\},$$

with

$$B=\int_0^{x_1}\left[\frac{p_i\xi}{x_1}\cos\frac{p_ix}{x_1}+\sin\frac{p_ix}{x_1}\right]\frac{p_0(0)\exp(-\alpha x)}{k_1/N+x}dx, \qquad (12)$$

$$\xi=\left[\frac{K_1}{D}+\frac{N}{k_1}\right]^{-1}.$$

L is the hole bulk diffusion length. The eigenvalues p_i, $i=1, 2, \cdots$ are the positive roots of

$$\frac{\tan p_i}{p_i}=-\frac{\xi}{x_1}. \qquad (13)$$

The total number of holes trapped per cm² of surface area per flash of uv is

$$\Delta p^+=K_1\int_0^{\infty}p_0dt=2\xi\frac{K_1k_1}{x_1DN}\sum_{i=1}^{\infty}(Bp_i/x_1)\Big/\left[\frac{p_i^2}{x_1^2}+L^{-2}\right]\left[1+\frac{2\xi}{x_1}+\frac{p_i^2\xi}{x_1^2}-\left(\frac{p_i^2\xi^3}{x_1^3}+\frac{\xi}{x_1}\right)\cos^2p_i\right]. \qquad (14)$$

According to (13), $(i-\frac{1}{2})\pi<p_i<i\pi$ and p_i can be approximated well by $i\pi$ if $i\leq x_1/10\xi\pi$. As one may still dispose of x_1, it can be made large without limit and the relative error of $\pi/2$ in $p_i\xi/x_1$ of (14) becomes small without limit. As the integrand of B becomes negligibly small for $\alpha x>10$, where α is a constant, we can make the values of x/x_1 for which the integrand contributes to the integral small without limit, and accordingly a negligible error is introduced in the sine and cosine expressions in B by the possible error of $\pi/2$ introduced into p_i if we let $p_i=i\pi$. Furthermore the term with $\cos^2p_i$ in the denominator of (14) can be neglected with respect to $1+(p_i^2\xi^2/x_1^2)$, and consequently substitution of $p_i=i\pi$ in (14) is a good approximation for all values of i. Accordingly,

$$\Delta p^+=\frac{2\xi p_0(0)K_1k_1}{DN\pi}\times\lim_{x_1\to\infty}\sum_{i=1}^{\infty}\left\{\frac{i\pi}{x_1}\left[-\xi\cos\frac{i\pi x}{x_1}+\sin\frac{i\pi x}{x_1}\right]\Big/\left[\frac{i^2\pi^2}{x_1^2}+L^{-2}\right]\left[1+\frac{i^2\pi^2\xi^2}{x_1^2}\right]\right\}\times\int_0^{x_1}\frac{\exp(-\alpha x)dx}{k_1/N+x}\left(\frac{\pi}{x_1}\right),$$

or

$$\Delta p^+=\frac{2\xi p_0(0)K_1k_1}{DN\pi}(I_1+\xi I_2),$$

where

$$I_1=\int_0^{\infty}\frac{\exp(-\alpha x)dx}{k_1/N+x}\int_0^{\infty}\frac{z\sin zxdz}{(z^2+L^{-2})(1+z^2\xi^2)},$$

and

$$I_2=\lim_{A\to\infty}\int_0^{\infty}\frac{\exp(-\alpha x)dx}{k_1/N+x}\int_0^{A}\frac{z^2\cos zxdz}{(z^2+L^{-2})(1+z^2\xi^2)}.$$

This leads after evaluation of I_1 and I_2 and by using (12) to

$$\frac{\Delta p^+}{\Delta q}=\frac{K_1\alpha\gamma\exp\gamma}{D(\alpha+L^{-1})[(K_1/D)+L^{-1}+\gamma^{-1}(\alpha+L^{-1})]}\times\int_{\gamma}^{\infty}\frac{\exp(-z)}{z}dz, \qquad (15)$$

$$\gamma=\frac{(\alpha+L^{-1})k_1}{N} \quad \text{and} \quad \Delta q=\int_0^{\infty}p_0(0)\exp(-\alpha x)dx=\frac{p_0(0)}{\alpha}$$

is the total number of holes created by one flash of light per unit of surface area. $\Delta p^+/\Delta q$ is the quantum efficiency of the surface charge producing process.

Equation (15) is of course valid only if the sample is large enough with respect to the diffusion length of holes to prevent these from diffusing across the crystal to the other side which appears to be the case as shown in Appendix I. The fact that holes do not diffuse across the crystal was used in deriving (15) when $x_1 \rightarrow \infty$. Furthermore (11) should hold in the region near the surface from which holes can reach the surface. There is some doubt that this is so for small positive surface potentials. However (11) holds again exactly for a neutral surface.

Numerical integration of (15) yields

$$q=\int_0^{p+} \frac{D(\alpha+L^{-1})[(K_1/D)+L^{-1}+\gamma^{-1}(\alpha+L^{-1})]}{K_1\alpha\gamma \exp(\gamma)\int_\gamma^\infty \exp(-z)dz/z} d\zeta, \tag{16}$$

with

$$\gamma=(\alpha+L^{-1})k_1 \Big/ \int_0^\zeta \frac{\mu_f}{\mu_m} dp^+,$$

μ_m is the electron micromobility and p^+, q, and μ_f have been defined before.

PHYSICAL REVIEW VOLUME 114, NUMBER 3 MAY 1, 1959

Optical Properties of Tellurium and Selenium*

ROBERT S. CALDWELL† AND H. Y. FAN
Purdue University, Lafayette, Indiana
(Received December 15, 1958)

The optical properties of tellurium and of trigonal and amorphous selenium have been investigated at wavelengths extending from the intrinsic absorption edge to about 152 microns using polarized radiation. The refractive indices of tellurium and trigonal selenium have been determined from 4 to 14 microns and from 9 to 23 microns, respectively. For amorphous selenium, the refractive index estimated from measured reflectivity shows no appreciable variation from 30 to 152 microns. The temperature shift and the pressure shift of the intrinsic absorption edge in amorphous selenium are found to be -1.45×10^{-3} ev/°K and -2.0×10^{-5} ev/atmos, respectively. Lattice absorption bands have been observed in tellurium and selenium; they are attributed to the excitation of combination modes. In tellurium, a strong absorption band has been observed at 11 microns, which is present only for $E\|c$ radiation. The band indicates that there are overlapping branches in the valence band which are separated by about 0.11 ev. The effective mass in the lower branch is estimated to be about four times smaller than that in the upper branch. It is possible that the structure of the valence band is responsible for the high-temperature reversal of the Hall effect in tellurium. The usual carrier absorption increasing smoothly with wavelength has been studied for tellurium using polarized radiations. The effective mass of holes in tellurium has been determined from reflectivity measurements: $m_\perp \sim m_{\|}=0.45\ m$ at 300°K, $m_\perp=0.30\ m$ and $m_{\|}=0.45\ m$ at 100°K.

I. INTRODUCTION

THE investigation of the optical properties of semiconductors has been very fruitful for the understanding of the materials. Tellurium and selenium are two elemental semiconductors, the optical properties of which have not yet been studied as extensively as in some other cases. The fact that these crystals are not cubic in structure and are birefringent makes the optical properties more interesting.

The crystal structure of tellurium consists of parallel spiral chains arranged at the corners and the center of a hexagon. The direction of the chains is the c axis of the crystal. Every third atom in a chain completes one revolution of the spiral, so that the projection of the atoms on a plane perpendicular to the chain axes consists of equilateral triangles. The distance from an atom to the two nearest neighbors, which are in the same chain, is 2.86 A, while the distance to the four second nearest neighbors, which are in adjacent chains, is 3.46 A. Thus the binding between atoms in a chain is stronger than the binding between the chains with the result that the material cleaves readily parallel to the c axis. The crystal has D_3 point group symmetry and belongs to the trigonal system. The primitive unit cell contains three atoms.

Selenium can exist in various allotropic forms. The trigonal crystalline form is the most stable and has the same structure as described above for tellurium but with smaller lattice constants, the nearest and second nearest neighbor distances being 2.32 A and 3.46 A, respectively. The two other crystalline forms which are monoclinic will not be dealt with in this work. Amorphous selenium, which is fairly stable below 50°C but converts to the trigonal form at higher temperatures, is of interest since it is characterized by the chain structure; x-ray measurements showed that the chain structure persists in the liquid phase of selenium and tellurium.[1]

* Work supported by a Signal Corps Contract.
† Now at Boeing Airplane Company, Seattle, Washington.

[1] R. C. Buschert, Ph.D. thesis, Purdue University, 1956 (unpublished).